

SVD-Aided UKF for Estimation of Nanosatellite Rotational Motion Parameters

DEMET CILDEN-GULER*, HALIL ERSIN SOKEN**, CHINGIZ HAJIYEV*,

*Faculty of Aeronautics and Astronautics
Istanbul Technical University
Maslak, 34469, Istanbul
TURKEY

cilden@itu.edu.tr, cingiz@itu.edu.tr,

**Institute of Space and Astronautical Science (ISAS)
Japan Aerospace Exploration Agency (JAXA)
Kanagawa, JAPAN
ersin_soken@ac.jaxa.jp

Abstract: - Singular Value Decomposition (SVD) and unscented Kalman filter (UKF) are interlaced using the Euler angles as the attitude parameter in order to estimate the satellite's angular motion parameters about center of mass. Magnetometer and sun sensor are used as the vector measurements for SVD in addition to the angular rate measurements from rate gyro for UKF; therefore, the output of the SVD shaped the nontraditional approach as SVD-aided UKF algorithm using the linear measurements.

Key-Words: - Satellite attitude estimation, magnetometer, sun sensor, rate gyro, unscented Kalman filter, angular velocity, nontraditional approach.

1 Introduction

Cooperating magnetometer sun sensor and rate gyro utilization in small satellite missions is a common method for achieving accurate attitude information. By the use of a Kalman filter algorithm measurement inputs of these sensors can be easily integrated in order to estimate the attitude parameters of the satellite precisely. At this stage, the methods of dynamic filtration (for example Kalman filters) may be useful.

The traditional approaches to design of Kalman filter for satellite attitude and rate estimation use the nonlinear measurements of reference directions [1]–[6]. In nontraditional approach based attitude estimation (based on linear measurements) attitude angles are found by vector measurements at each step. Then these are directly used as measurement input for Kalman filter [7]–[14]. Hence measurement model is linear in this case, since the states are measured directly. In [15], the papers using different kinds of approaches are reviewed.

Integration of single-frame satellite attitude determination methods with Kalman filter is presented by [7], [8], in which the algebraic method and EKF algorithms are combined to estimate the attitude angles and angular velocities respectively.

Attitude determination system use algebraic method (2-vector algorithm). This method is based on the computing any two analytical vectors in the reference frame and measuring these vectors in the body coordinated system [16]. As measuring devices magnetometers, Sun sensors, and horizon scanners/sensors are used. Three different algorithms based on Earth's magnetic field, Sun vector, and nadir vector are used. In order to obtain the attitude of the satellite with desired accuracy an EKF for satellite's angular motion parameter estimation is designed. In [14], it is stated that the integrated SVD/EKF can achieve more accurate attitude results than the traditional approach because of its adaptive way for the covariance values.

In this study, an attitude estimation algorithm based on the SVD-aided UKF nontraditional approach is proposed. The proposed prediction algorithm is stepped in for better attitude estimation of the satellite. The absolute errors of attitude determination and estimation of the satellite's rotational motion parameters are investigated.

The structure of this paper is as follows. Section 2 gives the attitude determination using the vector measurements including the mathematical models and SVD method. SVD/UKF for satellite attitude estimation based on linear measurements

(nontraditional approach), and their simulation results are presented in Section 3 and 4 respectively. Finally, the Section 5 gives a brief summary of the obtained results and conclusions.

2 Attitude Determination using Vector Measurements

2.1 Mathematical Models and Vector Measurements

If the kinematic equations of the small satellite are derived according to Euler's angles, then the mathematical model can be expressed. Here, 7-dimensional state vector orientation angles (φ roll - x axis; θ pitch - y axis; ψ yaw - z axis), contains the angular velocities and the inertial moment on the y -axis.

$$\bar{x} = [\varphi \quad \theta \quad \psi \quad \omega_x \quad \omega_y \quad \omega_z]^T. \quad (1)$$

Angular velocities for consistency are expressed in the body axis set according to the inertial coordinate system.

$$\bar{\omega}_{BI} = [\omega_x \quad \omega_y \quad \omega_z]^T, \quad (2)$$

Here, $\bar{\omega}_{BI}$ represents the angular velocities of the body axis set. Dynamic equations are also obtained by the principle of conservation of angular momentum.

$$J_x \frac{d\omega_x}{dt} = N_x + (J_y - J_z)\omega_y\omega_z, \quad (3)$$

$$J_y \frac{d\omega_y}{dt} = N_y + (J_z - J_x)\omega_z\omega_x, \quad (4)$$

$$J_z \frac{d\omega_z}{dt} = N_z + (J_x - J_y)\omega_x\omega_y, \quad (5)$$

J_x , J_y and J_z inertial moments, N_x , N_y and N_z is used for external disturbances affecting the satellite. If only the effect of gravity is taken into consideration, the external torques can be found as follows.

$$\begin{bmatrix} N_x \\ N_y \\ N_z \end{bmatrix} = -3 \frac{\mu}{r_0^3} \begin{bmatrix} (J_y - J_z)A_{23}A_{33} \\ (J_z - J_x)A_{13}A_{33} \\ (J_x - J_y)A_{13}A_{23} \end{bmatrix}. \quad (6)$$

μ gravitational constant, r_0 distance between Earth and satellite, A_{ij} represents the elements of the cosine matrix.

$$A = \begin{bmatrix} c(\theta)c(\psi) & c(\theta)s(\psi) & -s(\theta) \\ -c(\varphi)s(\psi) + s(\varphi)s(\theta)c(\psi) & c(\varphi)c(\psi) + s(\varphi)s(\theta)s(\psi) & s(\varphi)c(\theta) \\ s(\varphi)s(\psi) + c(\varphi)s(\theta)c(\psi) & -s(\varphi)c(\psi) + c(\varphi)s(\theta)s(\psi) & c(\varphi)c(\theta) \end{bmatrix}. \quad (7)$$

In A matrix, $c(\cdot)$ and $s(\cdot)$ are cosine and sinus functions. Thus, kinematic equations can be expressed in terms of Euler angles as follows.

$$\begin{bmatrix} \dot{\varphi} \\ \dot{\theta} \\ \dot{\psi} \end{bmatrix} = \begin{bmatrix} 1 & s(\varphi)t(\theta) & c(\varphi)t(\theta) \\ 0 & c(\varphi) & -s(\varphi) \\ 0 & s(\varphi)/c(\theta) & c(\varphi)/c(\theta) \end{bmatrix} \begin{bmatrix} p \\ q \\ r \end{bmatrix}. \quad (8)$$

$t(\cdot)$ is the tangent function and p , q , r are the components of the $\bar{\omega}_{BR}$ vector. $\bar{\omega}_{BI}$ and $\bar{\omega}_{BR}$ have the relationship as,

$$\bar{\omega}_{BR} = \bar{\omega}_{BI} + A \begin{bmatrix} 0 \\ -\omega_o \\ 0 \end{bmatrix} \quad (9)$$

ω_o orbital angular velocity in the equality of $\omega_o = (\mu/r_0^3)^{1/2}$.

The body angular rate vector with respect to the inertial axis is measured by the onboard gyros. Widely used model for the gyro measurements is

$$\tilde{\omega}_{BI} = \bar{\omega}_{BI} + \eta_g, \quad (10)$$

where, $\tilde{\omega}_{BI}$ is the measured angular rates of the satellite, and η_g is the zero mean Gaussian white noise with the characteristic of,

$$E[\eta_g(t_1)\eta_g^T(t_2)] = I_{3 \times 3} \sigma_g^2 \delta(t_1 - t_2) \quad (11)$$

Here, $I_{3 \times 3}$ is the 3×3 unit matrix, σ_g is the standard deviation of each gyro random error and $\delta(t)$ is the Dirac delta function.

Magnetometer measurements and their corresponding models can be represented by assuming that magnetometer calibration has been already done with one of the in-orbit or on-ground estimation methods,

$$B_{mes} = \begin{bmatrix} B_x(\Phi, t) \\ B_y(\Phi, t) \\ B_z(\Phi, t) \end{bmatrix} = A \begin{bmatrix} B_1(t) \\ B_2(t) \\ B_3(t) \end{bmatrix} + \eta_m \quad (12)$$

where $B_1(t)$, $B_2(t)$ and $B_3(t)$ represent the Earth magnetic field vector components in the orbit frame; $B_x(\Phi, t)$, $B_y(\Phi, t)$ and $B_z(\Phi, t)$ show the measured

Earth magnetic field vector components in the body frame as a function of time and varying Euler angles vector. η_m is the zero mean Gaussian white noise with the characteristic of

$$E[\eta_m(t_1)\eta_m^T(t_2)] = I_{3 \times 3} \sigma_m^2 \delta(t_1 - t_2), \quad (13)$$

σ_m is the standard deviation of each magnetometer error.

One of well-known methods for obtaining the Earth magnetic field vector components in the orbit frame is using the International Geomagnetic Reference Field (IGRF) model. The selected IGRF-12 model uses predictive secular variation coefficients for 2015-2020 period [18].

Sun direction in the Earth Centered Inertial (ECI) frame can be modelled in terms of the Julian Day (T_{TDB}) which is defined using the satellite's reference epoch and the exact time. We first calculate the ecliptic longitude of the Sun ($\lambda_{ecliptic}$) and the linear model of the ecliptic longitude of the Sun (ε)¹¹. Then we can get, the unit Sun direction vector (S_{ECI}) in ECI frame as.

$$S_{ECI} = \begin{bmatrix} \cos \lambda_{ecliptic} \\ \sin \lambda_{ecliptic} \cos \varepsilon \\ \sin \lambda_{ecliptic} \sin \varepsilon \end{bmatrix}. \quad (14)$$

Orbital elements from the orbit propagation model of the satellite are necessary for transforming the unit vector in ECI frame into the orbital frame. After that the model for the sun sensor measurements can be given as,

$$S_{mes} = S_b = AS_o + \eta_s, \quad (15)$$

where, S_o is the sun direction vector in the orbit frame and S_b are the sun sensor measurements in body frame which are corrupted with, η_s , the zero mean Gaussian white noise with the characteristic of

$$E[\eta_s(t_1)\eta_s^T(t_2)] = I_{3 \times 3} \sigma_s^2 \delta(t_1 - t_2). \quad (16)$$

where σ_s is the standard deviation of sun sensor error.

2.2 Singular Value Decomposition (SVD)

One of the most robust point-by-point methods that we can use for solving the Wahba's problem is the SVD method. The problem is to find the optimal solution for attitude transformation matrix A with

determinant of +1 that minimizes the loss function[3], [19]

$$L(A) = \frac{1}{2} \sum_i a_i |\mathbf{b}_i - A\mathbf{r}_i|^2, \quad (17)$$

where \mathbf{b}_i and \mathbf{r}_i are set of unit vectors obtained in two different coordinates. In this paper, these unit vectors represent sun direction and magnetic field in satellite orbit frame (\mathbf{r}_i) and body frame (\mathbf{b}_i). a_i is non-negative weight for each unit vector observations and can be selected as the inverse of the variance of measurement errors, σ_s^{-2} and σ_m^{-2} for sun sensor and magnetometer measurements respectively. We can write Eq. (17) in a more convenient form as,

$$L(A) = \lambda_0 - \text{tr}(AB^T), \quad (18)$$

where,

$$\lambda_0 = \sum a_i, \quad (19)$$

$$B = \sum a_i \mathbf{b}_i \mathbf{r}_i^T. \quad (20)$$

Hence, the cost function minimization problem reduces into the problem of maximizing the trace, $\text{tr}(AB^T)$. There are many single frame methods for solving this problem. The SVD is one of the most accurate, reliable and robust methods amongst them¹². The matrix B has singular value decomposition:

$$B = U \Sigma^T V^T = U \text{diag}[\Sigma_{11} \quad \Sigma_{22} \quad \Sigma_{33}] V^T \quad (21)$$

where U and V are orthogonal and the singular values that obey $\Sigma_{11} \geq \Sigma_{22} \geq \Sigma_{33} \geq 0$. Then we can show that the trace is maximized for Eq.(22) and optimal transformation matrix can be obtained as Eq.(23).

$$U^T A_{opt} V = \text{diag}[1 \quad 1 \quad \det(U)\det(V)] \quad (22)$$

$$A_{opt} = U \text{diag}[1 \quad 1 \quad \det(U)\det(V)] V^T \quad (23)$$

The accuracy of the estimated A_{opt} can be evaluated by examining the covariance matrix for rotation angle error. If secondary singular variables are defined as, $s_1 = \Sigma_{11}$, $s_2 = \Sigma_{22}$, $s_3 = \det(U)\det(V)\Sigma_{33}$ then the covariance matrix P_{svd} is calculated as,

$$P_{svd} = U \text{diag}[(s_2 + s_3)^{-1} \quad (s_3 + s_1)^{-1} \quad (s_1 + s_2)^{-1}] U^T. \quad (24)$$

In this study, the satellite has two absolute sensors (e.g. sun, and magnetic field sensors), therefore the SVD-method fails when the satellite is in eclipse and two vectors are parallel. In the eclipse period, attitude estimations may become reliable if the described SVD method is integrated with a recursive filtering algorithm as it is discussed in the following section.

3 Attitude Estimation using Nontraditional Approach (SVD-Aided UKF)

The SVD method and UKF can be integrated for having more accurate attitude estimates. Using vector measurements at a single time, the SVD estimates the attitude, while the UKF incorporates the spacecraft dynamics/kinematics information and gyro measurements to achieve better estimation performance. The combined SVD/UKF method filters and increases the accuracy of the attitude estimations coming from the SVD.

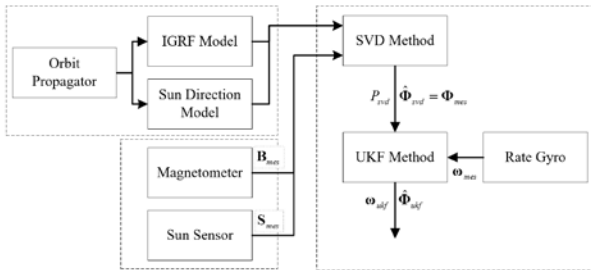


Fig. 1. SVD/UKF attitude estimation scheme.

Two methods are integrated by treating the attitude estimations coming from the SVD method as the Euler angle vector measurements for the UKF. The measurement covariance matrix for the UKF, R , is obtained by processing the P_{svd} , the covariance matrix for rotation angle errors.

The scheme for the integrated SVD/UKF method is given in Fig.1. At the beginning, the SVD method provides the attitude estimations in Euler angles (Φ_{svd}) using magnetometer (B_{mes}) and sun sensor (S_{mes}) measurements. In addition to have the dynamic mathematical model of the satellite's rotational motion, the rate gyro measurements (ω_{mes}) are used in order to estimate the angular

velocity of the nanosatellite. So, together with the gyro measurements (ω_{mes}), angle determinations from SVD are used as measurement inputs to the UKF.

The mathematical expressions for UKF can be given. The essence of the UKF is the unscented transform, a deterministic sampling technique that we use for obtaining a minimal set of sample points (or sigma points) from the *a priori* mean and covariance of the states. These sigma points go through a nonlinear transformation. The posterior mean and the covariance are determined using the transformed sigma point [5].

The UKF is derived for discrete-time nonlinear equations, so the system model is given by;

$$x(k+1) = f(x(k), k) + w(k), \quad (25a)$$

$$y(k) = Hx(k) + v(k). \quad (25b)$$

Here, $x(k)$ is the state vector and $y(k)$ is the measurement vector. Moreover $w(k)$ and $v(k)$ are the process and measurement error noises, which are assumed to be Gaussian white noise processes with the covariance of $Q(k)$ and $R(k)$ respectively, H is the measurement matrix.

The initial step of the UKF algorithm is determining the $2n+1$ sigma points with a mean of $\hat{x}(k|k)$ and a co variance of $P(k|k)$. For an n -dimensional state vector, these sigma points are obtained by

$$x_0(k|k) = \hat{x}(k|k), \quad (26a)$$

$$x_\gamma(k|k) = \hat{x}(k|k) + \left(\sqrt{(n+\kappa)P(k|k)} \right)_\gamma, \quad (26b)$$

$$x_{\gamma+n}(k|k) = \hat{x}(k|k) - \left(\sqrt{(n+\kappa)P(k|k)} \right)_\gamma, \quad (26c)$$

where, $x_0(k|k)$, $x_\gamma(k|k)$ and $x_{\gamma+n}(k|k)$ are sigma points, n is the state number, and κ is the scaling parameter which is used for fine tuning. $\left(\sqrt{(n+\kappa)P(k|k)} \right)_\gamma$ corresponds to the γ^{th} column of the indicated matrix and γ is given as $\gamma = 1 \dots n$.

The next step of the UKF procedure is evaluating the transformed set of sigma points for each of the points by,

$$x_l(k+1|k) = f[x_l(k|k), k]. \quad l = 0 \dots 2n \quad (27)$$

Thereafter, these transformed values are utilised for gaining the predicted mean and covariance [11].

$$\hat{\mathbf{x}}(k+1|k) = \frac{1}{n+\kappa} \left\{ \kappa \mathbf{x}_0(k+1|k) + \frac{1}{2} \sum_{i=1}^{2n} \mathbf{x}_i(k+1|k) \right\}, \quad (28a)$$

$$P(k+1|k) = \frac{1}{n+\kappa} \times \left\{ \kappa [\mathbf{x}_0(k+1|k) - \hat{\mathbf{x}}(k+1|k)] \times [\mathbf{x}_0(k+1|k) - \hat{\mathbf{x}}(k+1|k)]^T + \frac{1}{2} \sum_{i=1}^{2n} [\mathbf{x}_i(k+1|k) - \hat{\mathbf{x}}(k+1|k)] [\mathbf{x}_i(k+1|k) - \hat{\mathbf{x}}(k+1|k)]^T \right\} + Q(k) \quad (28b)$$

Here, $\hat{\mathbf{x}}(k+1|k)$ is the predicted mean and $P(k+1|k)$ is the predicted covariance. Furthermore, the predicted observation vector is,

$$\hat{y}(k+1/k) = H(k+1)\hat{\mathbf{x}}(k+1/k). \quad (29)$$

After that, the observation covariance matrix is determined as,

$$P_{yy}(k+1/k) = H(k+1)P(k+1/k)H^T(k+1), \quad (30)$$

On the other hand, the cross-correlation matrix can be obtained as,

$$P_{xy}(k+1/k) = P(k+1/k)H^T(k+1) \quad (31)$$

Following part is the update phase of UKF algorithm. At that phase, first by using measurements, $y(k+1)$, the residual term (or innovation sequence) $\nu(k+1)$ is found as the difference between the actual observation and the predicted observation:

$$\nu(k+1) = y(k+1) - \hat{y}(k+1|k), \quad (32)$$

The innovation covariance is,

$$P_{vv}(k+1|k) = P_{yy}(k+1|k) + R(k+1) = H(k+1)P(k+1/k)H^T(k+1) + R(k+1) \quad (33)$$

Here, $R(k+1)$ is the measurement noise covariance matrix. Kalman gain is computed via equation of,

$$K(k+1) = P_{xy}(k+1|k)P_{vv}^{-1}(k+1|k). \quad (34)$$

At last, updated states and covariance matrix are determined by,

$$\hat{\mathbf{x}}(k+1|k+1) = \hat{\mathbf{x}}(k+1|k) + K(k+1)\nu(k+1), \quad (35)$$

$$P(k+1|k+1) = P(k+1|k) - P_{xy}(k+1/k)P_{vv}^{-1}(k+1|k)P_{xy}^T(k+1/k). \quad (36)$$

$$P(k+1|k+1) = P(k+1|k) - K(k+1)P_{vv}(k+1|k)K^T(k+1) \quad (37)$$

Here, $\hat{\mathbf{x}}(k+1|k+1)$ is the estimated state vector and $P(k+1|k+1)$ is the estimated covariance matrix.

4 Simulation Results

Simulations are performed for evaluating the attitude determination algorithm for a hypothetical nanosatellite. The orbit of the satellite is assumed to be at Low Earth Orbit (LEO) with circular orbit.

For the magnetometer measurements, the sensor noise is characterized by zero mean Gaussian white noise with a standard deviation of $\sigma_m = 0.008$ and as mentioned we assume that the magnetometers are calibrated against sensor biases, scale factors etc. Moreover, the standard deviation for the sun sensor noise is taken as $\sigma_s = 0.002$ (for unit vector measurements) and the sun sensor is also calibrated against biases.

Algorithm runs for 1200 sec, and the whole algorithm including the SVD, models, and UKF is propagated with a sampling time of $\Delta t = 0.1s$.

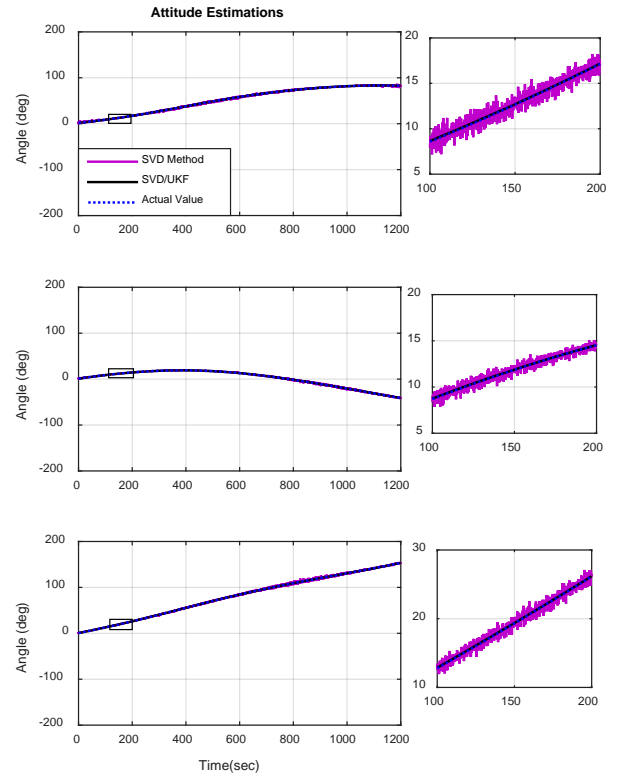


Fig. 2. Attitude estimation of the SVD, and SVD/UKF algorithm with respect to actual simulation values.

In Fig. 2, the estimations by SVD and SVD/UKF are given with the actual values. The differences between the estimations can be seen more clear from the zoomed interval next to each panel in Fig. 2. Fig. 3 demonstrates the estimation error changes in time for both methods. Here, SVD only method estimates the attitude angles of the nanosatellite about 5 deg accuracy. On the other hand, SVD/UKF seen in Fig. 4 has the capability to estimate the attitude under 0.2 de g. From those simulation results, it can be said that SVD/UKF can estimate the attitude angles accurately.

The measurement noise covariance (R) of the UKF which is taken same as the rotation angle estimation covariance of the SVD (P_{svd}), plays an important role for the estimations.

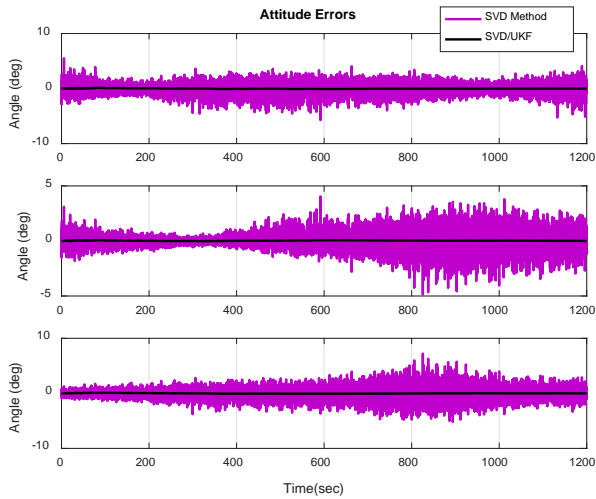


Fig. 3. Attitude estimation errors of SVD and SVD/UKF methods.

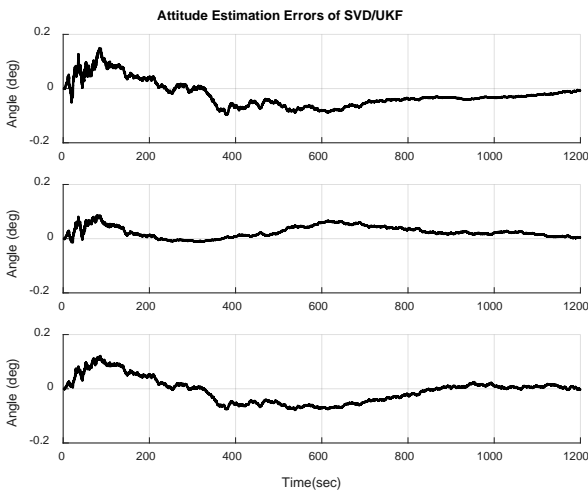


Fig. 4. Attitude estimation errors of SVD/UKF method.

The angular velocities of the nanosatellite are estimated by SVD/UKF and shown in Fig. 5 with the actual values. As also seen in Fig. 6, the presented algorithm estimates the angular rates accurately after about 180 s transient period.

All in all, the accuracy performance of the proposed filter is well for estimating both attitude and rates of the nanosatellite.

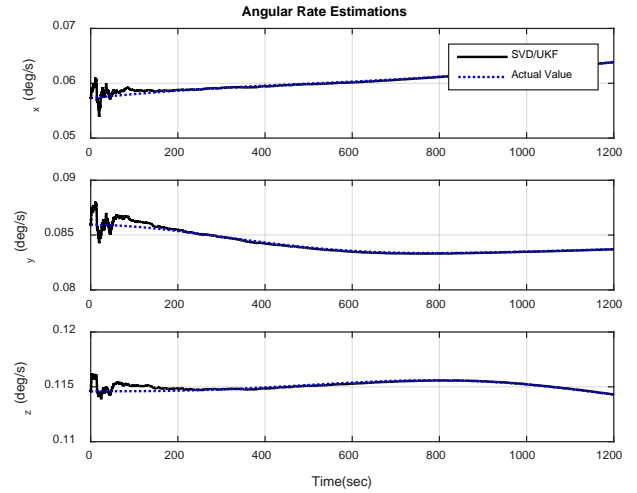


Fig. 5. Angular rate estimation of the SVD/UKF algorithm with respect to actual simulation values.

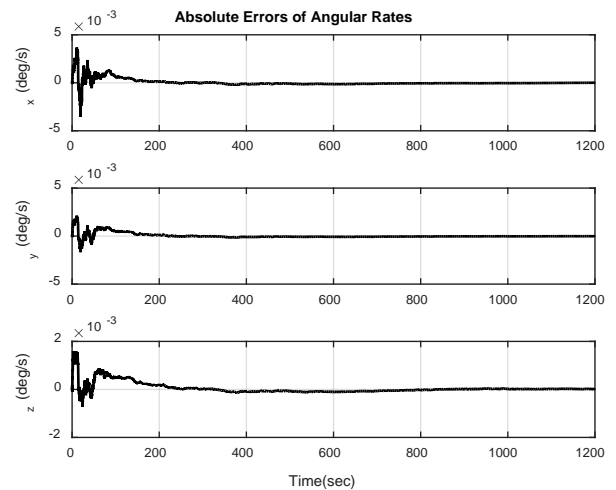


Fig. 6. Angular rate estimation errors of SVD/UKF method.

5 Discussion of SVD-Aided UKF Properties

Several properties of the proposed SVD-aided UKF attitude estimation algorithm are discussed in this section.

In the proposed approach, UKF is designed for the linear measurement equations. It reduces the

complexity of filter design and increase the accuracy. For this purpose, robustness against measurement faults and an eclipse period cases are considered.

An important advantage of the SVD-aided UKF algorithm in addition to having linear measurements is having the measurement variance updated at each estimation step which makes the filter adaptive. This causes an increase on the covariance matrix of measurement noise R if there is a fault on the measurement. The time series of the attitude estimations including an eclipse period (from 400 to 800 s correspond to the eclipse) is shown in Fig. 7. Here, the output of the Sun sensor is zero (zero output sensor fault occurs). Therefore, the diagonal elements of matrix R increase significantly (see Fig. 8).

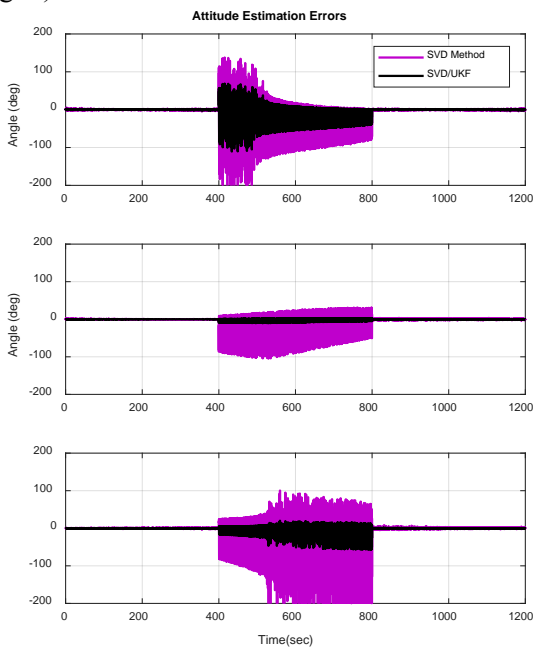


Fig. 7. Attitude estimation errors of the SVD, and SVD/UKF algorithm including an eclipse period.

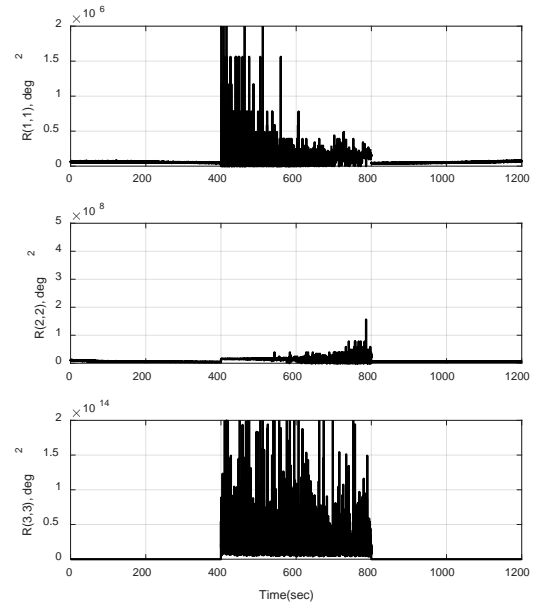


Fig. 8. Measurement noise covariance diagonal elements in case of zero output sensor fault.

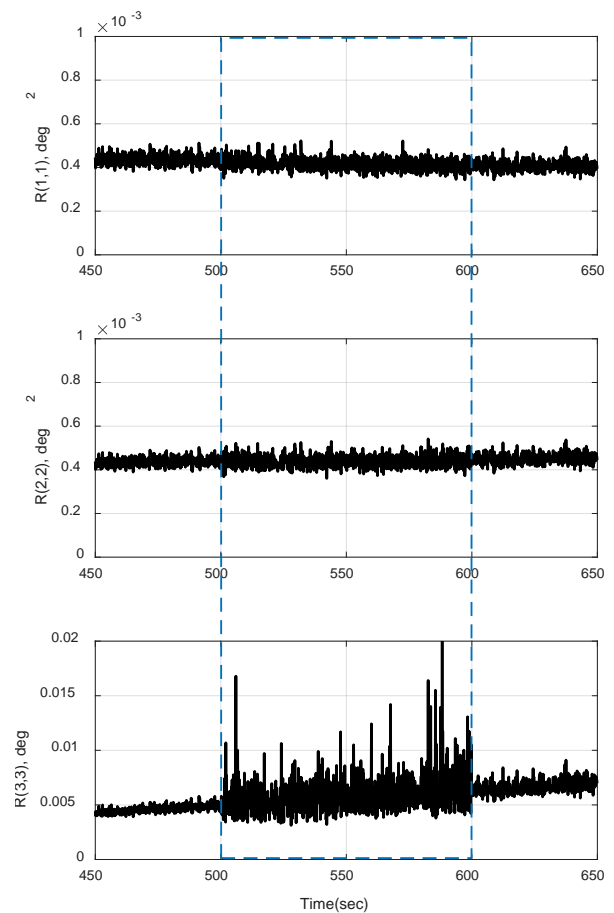


Fig. 9. Measurement noise covariance diagonal elements in case of noise increment sensor fault.

The next scenario is applying a noise increment on the magnetometer measurements. Magnetometer

measurement noises for each axis are increased 10 times between 500-600 s. The diagonal elements of the SVD-aided UKF measurement noise covariance matrix for this case are presented in Fig. 9. If a fault occur on the measurement system like here, R starts to oscillate (with an increased range for noise increment type of fault). As a result, the estimation errors of the attitude angles by SVD-aided UKF are not affected significantly as SVD does from the sensor fault and the algorithm works well in and after this period (see Fig. 10). However, it should be noted that if the period is not sufficiently short, as it was in our case, then it might cause gross estimation errors which are increasing in time.

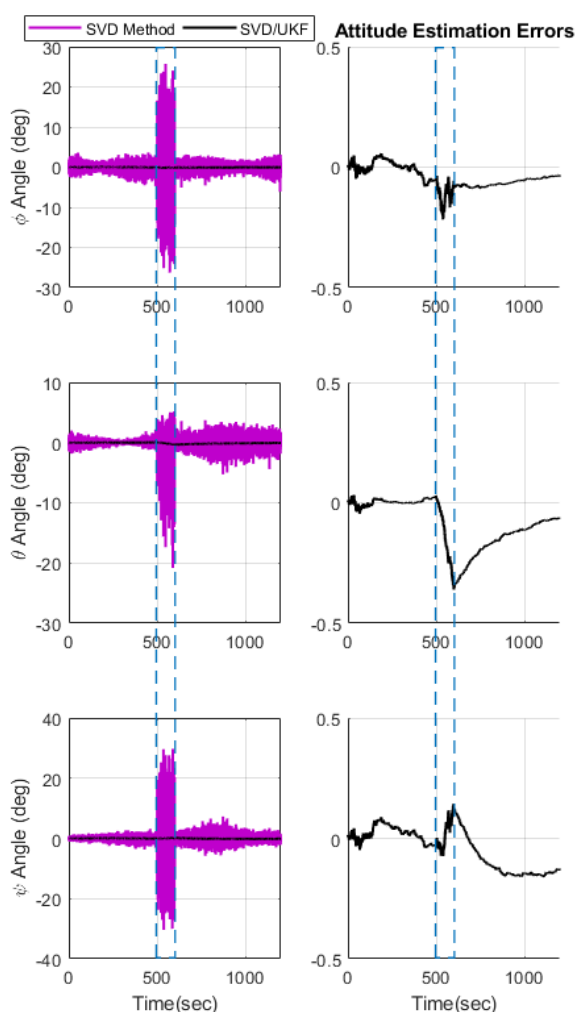


Fig. 10. Attitude estimation errors of the SVD, and SVD/UKF algorithm in case of noise increment sensor faults.

5 Conclusion

Singular Value Decomposition (SVD) method and Unscented Kalman Filter (UKF) are integrated to estimate the attitude and attitude rates for a nanosatellite. At the first phase, the SVD algorithm

estimates Euler angles. Then these estimates are used as measurement inputs for the UKF together with the gyro measurements. Demonstrations show that the SVD/UKF is capable to estimate the attitude angles and rates accurately. The properties of the presented algorithm are examined for zero-output and noise increment fault cases. It is concluded that the adaptive tuning of the SVD aided UKF provide the filter to be robust against measurement faults. For further studies, the attitude and rate estimation accuracies can be examined with considering only the kinematics model and without the dynamic model in the filter.

References

- [1] M. L. Psiaki, Three-axis attitude determination via Kalman filtering of magnetometer data, *J. Guid. Control Dyn.*, vol. 13, no. 3, 1989, pp. 506–514.
- [2] P. Sekhavat, Q. Gong, and I. M. Ross, NPSAT I parameter estimation using unscented Kalman filter, in *Proc. 2007 American Control Conference*, 2007, pp. 4445–4451.
- [3] K. Vinther, K. F. Jensen, J. A. Larsen, and R. Wisniewski, Inexpensive Cubesat Attitude Estimation Using Quaternions And Unscented Kalman Filtering, *Autom. Control Aerosp.*, vol. 4, 2011.
- [4] C. Hajiyev and H. E. Soken, Robust adaptive unscented Kalman filter for attitude estimation of pico satellites, *Int. J. Adapt. Control Signal Process.*, vol. 28, no. 2, 2014, pp. 107–120.
- [5] H. E. Soken, C. Hajiyev, and S. Sakai, Robust Kalman Filtering for Small Satellite Attitude Estimation in the Presence of Measurement Faults, *Eur. J. Control*, vol. 20, 2014, pp. 64–72.
- [6] H. E. Soken and C. Hajiyev, UKF for the identification of the pico satellite attitude dynamics parameters and the external torques on I MU and magnetometer measurements, in *4th International Conference on Recent Advances in Space Technologies*, 2009, pp. 547–552.
- [7] C. Hajiyev and M. Bahar, Multichannel Kalman Filter Based on Preliminary Data

- Compression for the Satellite Rotational Motion Parameters Identification, in *Proc. of the 3rd International Conference on Nonlinear Problems in Aviation and Aerospace*, vol. 1, 2000, pp. 277–284.
- [8] C. Hajiyev and M. Bahar, Attitude Determination and Control System Design of the ITU-UUBF LEO 1 Satellite, *Acta Astronaut.*, vol. 52, no. 2–6, 2003, pp. 493–499.
- [9] X. Yun and E. R. Bachman, Design, Implementation, and Experimental Results of a Quaternion-Based Kalman Filter for Human Body Motion Tracking, *IEEE Trans. Robot.*, vol. 22, no. 6, 2006, pp. 1216–1227.
- [10] B. Y. Mimasu and J. C. Van der Ha, Attitude determination concept for QSAT, *Trans. Japan Soc. Aeronaut. Sp. Sci. Aerosp. Technol. Japan*, vol. 7, 2009, pp. 63–68.
- [11] W. Quan, L. Xu, H. Zhang, and J. Fang, Interlaced Optimal-REQUEST and unscented Kalman filtering for attitude determination, *Chinese J. Aeronaut.*, vol. 26, no. 2, 2013, pp. 155–449.
- [12] D. Cilden, C. Hajiyev, and H. E. E. Soken, *Attitude and Attitude Rate Estimation for a Nanosatellite Using SVD and UKF (Accepted)*. Istanbul, Turkey, 2015, pp. 695–700.
- [13] C. Hajiyev and D. Cilden, Integrated SVD/EKF for Small Satellite Attitude and Rate Estimation, in *6th European Conference for Aeronautics and Space Sciences (EUCASS)*, 2015, p. 8P.
- [14] C. Hajiyev, D. Cilden, and Y. Somov, Gyro-free attitude and rate estimation for a small satellite using SVD and EKF, *Aerosp. Sci. Technol.*, vol. 55, 2016, pp. 324–331.
- [15] C. Hajiyev and D. Cilden Guler, Review on gyroless attitude determination methods for small satellites, *Prog. Aerosp. Sci.*, vol. 90, 2017, pp. 54–66.
- [16] J. R. Wertz, *Spacecraft Attitude Determination and Control*, no. 73. Dordrecht, Holland: Kluwer Academic Publishers, 1988.
- [17] C. Hajiyev and D. Cilden, Nontraditional Approach to Satellite Attitude Estimation, *Int. J. Control Syst. Robot.*, vol. 1, 2016, pp. 19–28.
- [18] E. Thébault, C. C. Finlay, C. D. Beggan, P. Alken, and E. Al., International Geomagnetic Reference Field: the 12th generation, *Earth, Planets Sp.*, vol. 67, no. 1, 2015, p. 79.
- [19] G. Wahba, Problem 65-1: A Least Squares Estimate of Satellite Attitude, *Soc. Ind. Appl. Math. Rev.*, vol. 7, no. 3, 1965, p. 409.